Cardiovascular Innovations and Applications

Vol. 2 No. 1 (2017) 85–99
ISSN 2009-8618
DOI 10.15212/CVIA.2016.0058

REVIEW

Magnetic Resonance Imaging of Coronary Arteries: Latest Technical Innovations and Clinical Experiences

Yibin Xie, PhD[1], Jianing Pang, PhD[2], Qi Yang, MD[1] and Debiao Li, PhD[1,3]

[1]Biomedical Imaging Research Institute, Cedars Sinai Medical Center, Los Angeles, CA, USA
[2]Siemens Healthcare, Chicago, IL, USA
[3]Department of Bioengineering, University of California, Los Angeles, CA, USA

Received: 12 January 2017; Revised: 31 January 2017; Accepted: 1 February 2017

Abstract

Cardiovascular disease (CVD) is the leading cause of death and a major health care challenge globally. Coronary artery disease (CAD) is a primary underlying pathological process in the majority of cardiovascular disease cases. Magnetic resonance imaging (MRI) can play a potentially important role in the management of CAD as a noninvasive imaging modality without ionizing radiation, although its early promise has not been delivered because of several crucial technical limitations. However, recent innovations in MRI have reopened the door, with tremendous opportunities for multiparametric assessment of CAD including luminal stenosis, plaque burden and composition, and disease activities such as inflammation and hemorrhage. Novel MRI acquisition and reconstruction strategies now offer much increased spatial resolution and image quality and shortened examination times compared with conventional approaches. Recent clinical experiences of coronary MRI indicated the potential to improve the current management of coronary atherosclerosis, such as identifying the patients at the highest risk and evaluating therapeutic responses. In this review we discuss the latest technical advances and clinical insights in coronary MRI.

Keywords: magnetic resonance imaging; magnetic resonance angiography; coronary atherosclerosis; coronary vessel wall imaging

Introduction

Cardiovascular disease (CVD), including mainly heart disease and stroke, is the leading cause of death globally and a major economic burden. A recent World Health Organization report estimated 17.3 million deaths per year are due to CVD, a number that is expected to grow to more than 23.6 million by 2030 [1]. Decades of advances in the diagnostic and treatment methods have helped reduce deaths by heart disease in many developed countries. For instance, according to the American Heart Association, the heart disease death rate fell by about 38% from 2003 to 2013 in the United States, although heart disease remains the leading cause of death, killing more than 370,000 people annually [2]. More alarmingly, the prevalence of CVD in many low- to mid-income countries has increased significantly in recent years. China, for example, has the highest CVD death rates in the world, with CVD accounting

Correspondence: **Debiao Li**, PhD, Biomedical Imaging Research Institute, Cedars-Sinai Medical Center, 8700 Beverly Blvd., PACT Suite 800, Los Angeles, CA 90048, USA, Tel.: +1 (424) 672-5278, Fax: +1 (310) 248-8682, E-mail: debiao.li@cshs.org

for 45% of the total number of deaths [3]. Coronary artery disease (CAD) is the primary cause of heart disease. It results from coronary atherosclerosis, the hardening of arteries with the buildup of plaques in the coronary vessel wall. It is a slow, progressive pathophysiological process that typically takes decades of development before symptoms may occur. Atherosclerosis can lead to the narrowing of coronary arterial lumen, gradually reducing the blood flow to the myocardium. High-risk coronary plaques can rupture and trigger thrombus formation and sudden catastrophic blockage of the blood flow, often leading to myocardial infarction.

Imaging plays an important role in the diagnosis of CAD. Currently, X-ray computed tomography (CT) is the preferred noninvasive imaging modality for evaluation of CAD. X-ray CT has gained vast popularity in the clinic thanks to its fast acquisition, wide availability, and ease of standardization. Compared with X-ray CT, magnetic resonance imaging (MRI) has several key pros and cons for the assessment of CAD. First, it does not involve ionizing radiation, making it ideal for screening and serial imaging such as tracking therapeutic response. It is also a more attractive option to be used for younger patients. Second, it has multiple image contrast mechanisms – for instance, T1-weighted imaging, T2-weighted imaging, magnetic resonance angiography (MRA), and dark-blood imaging – making it versatile to evaluate multiple aspects of the lesion status, including luminal stenosis, plaque burden, and plaque composition. Lastly, coronary MRI can be complemented by other magnetic resonance (MR) examinations, such as myocardial perfusion and viability, making it a potential "one-stop" modality for a comprehensive assessment of CAD. However, despite being used increasingly more commonly for evaluation of the myocardium, MRI has yet to be adopted as a clinical imaging method to assess the coronary arteries. There are two major technical challenges limiting the clinical application of coronary MRI: the small size and the tortuous course of the arteries require high spatial resolution, ideally submillimeter in all three directions; the complex cardiac and respiratory motion in the coronary arteries necessitates sophisticated and often cumbersome gating schemes and setup. Therefore, conventional coronary MRI protocols are usually very long (>1 h) and image quality is patient and operator dependent.

Coronary MRI is progressing steadily toward delivering its early promise with continuous efforts to increase its speed, resolution, and reliability. The recent advent of groundbreaking MR innovations has opened up new possibilities for coronary MRI. In this review we will summarize the technical advances and clinical insights from recent coronary MRI developments with focus on both coronary MRA and vessel wall (plaque) imaging.

Coronary MRA

In the past decade, MRA has emerged as a promising noninvasive method for evaluation of luminal narrowing of coronary arteries. Because of the small caliber of the coronary vessels, continuous motion, and proximity to myocardium and fat, successful coronary MRA requires high-resolution 3D imaging, effective contrast generation, and motion suppression strategies. Current techniques typically achieve spatial resolution of 1.0–1.3 mm and prescribe imaging volumes that cover the entire heart. Contrast generation strategies include fat suppression [4], T2-prepared balanced steady-state free-precession (SSFP) sequence at 1.5 T [5], and inversion recovery–prepared spoiled gradient echo sequence with T1-shortening contrast at 3 T [6]. Current motion-suppression methods include prospective electrocardiogram (ECG) gating for cardiac motion, where the segmented data acquisition is triggered by the R wave and limited to the cardiac quiescent period [7, 8], and prospective navigator gating for respiratory motion, where a *k*-space segment is repeatedly acquired until the diaphragm position, determined by a separate navigator acquisition, falls within a predetermined window [9].

To date, coronary MRA remains a niche application clinically, available only in experienced academic centers. The outstanding challenges are threefold: first, the spatial resolution is relatively low and often anisotropic [10], limiting the confidence with which stenosis is diagnosed, as well as the visualization of distal segments and small branches; second, the imaging time is relatively long at 10–15 min with respiratory gating, which not only causes patient discomfort but may also result in drifts in diaphragm position, bulk motion, and heart rate variation, all of which may lead to degradation of image quality

and even failure to complete the scan; third, current protocols involve many steps that require a highly trained operator, including heart localization, cardiac quiescent window selection through cine scans, and navigator placement through multiple additional localizer scans.

To address these challenges, recent efforts have focused on combining non-Cartesian *k*-space trajectories, acceleration strategies, and advanced motion correction frameworks to increase spatial resolution, shorten acquisition time, and increase the robustness to motion. A number of authors have proposed the use of 3D projection reconstruction (3DPR) acquisition for whole-heart coronary MRA. As each *k*-space line passes through the *k*-space center, 3DPR is robust to motion, can tolerate moderate undersampling showing incoherent, noise-like aliasing artifacts, and covers a large field of view efficiently with high isotropic resolution. Further, 3DPR allows multiple images to be retrospectively reconstructed from subsets of the total acquired data. These subsets are often segmented on the basis of motion signal, and the resulting motion-resolved series are used for subsequent image-based motion correction. For example, Bhat et al. [11] proposed achieving 100% respiratory gating efficiency by segmenting an ECG-gated, free-breathing 3DPR dataset into multiple respiratory bins using a monitoring diaphragm navigator, extracting the respiratory motion information using affine transform, and combining all bins with image-space motion correction. Pang et al. [12] extended this concept by replacing the navigator with self-navigation and performing analytical *k*-space motion correction. Stehning et al. [13] and Piccini et al. [14] proposed acquiring an extra superior–inferior self-navigation line and performing beat-by-beat translational respiratory motion correction. Piccini et al. [15] proposed a retrospective respiratory gating strategy with 3DPR by keeping only one of the respiratory bins, and suppressing undersampling artifacts through exploitation of the correlation in the respiratory dimension. Other types of trajectories with similar properties have also been explored; for example, a 3D cones trajectory [16–18] and a 3D Cartesian with radial phase ordering [19]. To shorten the acquisition time, many acceleration techniques have been proposed, including compressed sensing (CS) and parallel imaging. Moghari et al. [20] proposed a hybrid navigator gating/monitor-only method that filled in missing *k*-space samples using CS. Akcakaya et al. [21] demonstrated that for submillimeter Cartesian whole-heart coronary MRA, CS provided superior performance over parallel imaging at high acceleration factors. Forman et al. [22] proposed a CS framework that incorporated nonrigid respiratory motion correction. Nam et al. [23] proposed a graphical processing unit implementation of CS reconstruction with 3DPR acquisition. Pang et al. [24] used motion-corrected non-Cartesian sensitivity encoding to suppress the streaking artifacts in undersampled 3DPR acquisition. Luo et al. [25] proposed using outer volume suppression in combination with T2 preparation to suppress the signal from the surrounding tissues and thereby reduce the required matrix size. A number of investigators have developed advanced motion compensation strategies to increase the imaging efficiency of coronary MRA and increase its robustness to motion artifacts. Most work has focused on respiratory motion, in which all respiratory phases are accepted during acquisition, and the respiratory motion between respiratory phases is retrospectively corrected with use of information directly derived from self-navigation projections [13, 14], from image-based navigators through interleaved acquisitions [16, 26], or from respiratory phase–resolved reconstruction from subsets of the imaging data [27, 28]. One-dimensional [13, 14] and multidimensional [17, 26, 29] translation, affine [27, 28, 30], and nonrigid [18, 22, 31, 32] motion models have been used. Such motion correction techniques significantly reduce the scan time and largely eliminate the scan time uncertainty compared with prospective navigator gating. Another class of methods is 4D coronary MRA, where *k*-space data are continuously acquired while the cardiac and respiratory motion information is recorded simultaneously through self-navigation alone [15, 33, 34] (Figures 1 and 2) or through both ECG and self-navigation [35]. Such an acquisition strategy offers a fixed scan time, enables the flexibility to retrospectively exclude motion outliers, and provides coronary artery assessment and left ventricle function information from a single scan. Pang et al. [36] also proposed increasing the retrospective cardiac gating efficiency of 4D coronary MRA by extending the cardiac acceptance window beyond a single

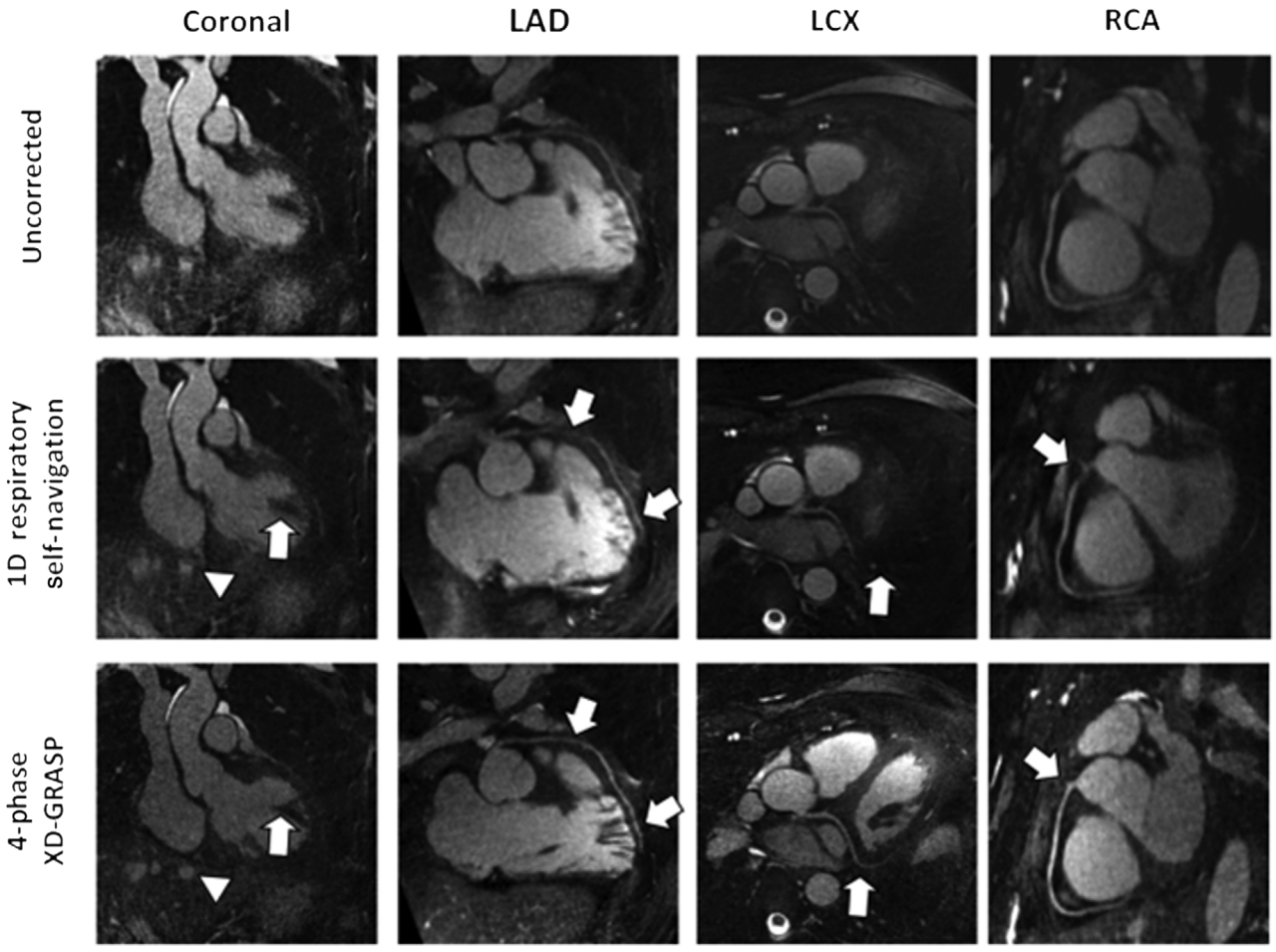

Figure 1 Example Images from Coronary Magnetic Resonance Angiography (MRA) with Extradimensional Golden-Angle Radial Sparse Parallel Imaging (XD-GRASP).
Example of a selected healthy adult volunteer dataset in which 1D respiratory self-navigation did not lead to diagnostic image quality. Although a clear improvement can be noticed from the uncorrected reconstruction to 1D respiratory self-navigation, the coronal view still shows strong residual blurring after conventional respiratory motion correction. Only the proximal segments of the left anterior descending artery (LAD) and the left circumflex coronary artery (LCX) are visible, whereas the right coronary artery (RCA), although visible, was not scored with full diagnostic quality in the mid and distal segments. By contrast, the dataset provided by the XD-GRASP reconstruction shows sharp and well-defined margins of a papillary muscle in the left ventricle and of the liver on the coronal view (*arrowheads*). All coronary arteries were better depicted, and increased vessel length could be seen with XD-GRASP reconstruction. Coronary segments graded as visible but nondiagnostic in the 1D respiratory self-navigation were considered diagnostic with the proposed XD-GRASP method (*arrows*). From Piccini et al. [15], with permission from Wiley.

quiescent period and performing nonrigid cardiac motion correction (Figure 3).

Balanced SSFP whole-heart coronary MRA has become the method of choice for coronary imaging at 1.5 T. Several single-center studies have evaluated the diagnostic performance of 1.5-T SSFP whole-heart coronary MRA for the detection of significant coronary artery stenoses. In a study by Sakuma et al. [37], whole-heart coronary MRA acquisition was successful in 34 (87.2%) of 39 patients. The sensitivity, specificity, accuracy, and positive and negative predictive values of whole-heart coronary MRA in the detection of significant stenoses in the major coronary arteries were 82% (14 of 17 arteries), 91% (39 of 43 arteries), 88% (53 of 60 arteries), 78% (14 of 18 arteries), and 93% (39 of 42 arteries) respectively. To further improve detection of CAD, they performed whole-heart coronary MRA in 131 patients by using an optimized acquisition window [38]. In this study of 131 patients, MRA acquisition was completed in 113 (86%) of 131 patients. In a patient-based analysis, the sensitivity, specificity,

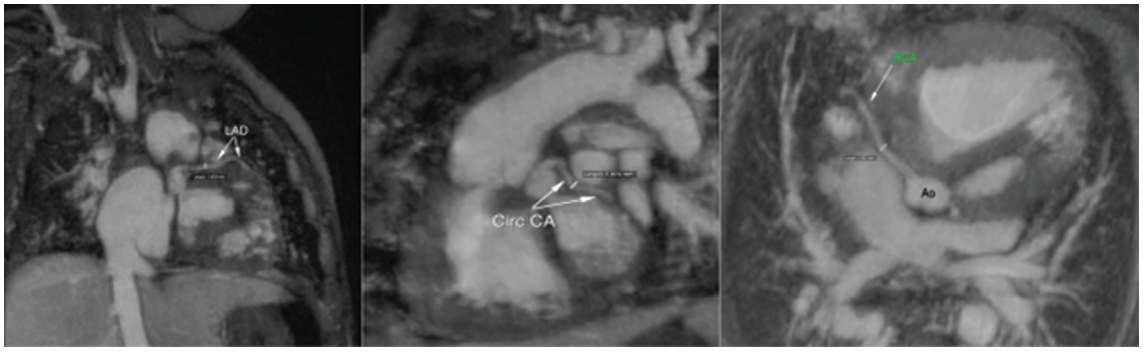

Figure 2 Example Images from Four-dimensional, Multiphase, Steady-state Imaging with Contrast Enhancement (4D MUSIC). All three major branches of the coronary artery (left anterior descending artery [LAD], left circumflex coronary artery [Circ CA], and right coronary artery [RCA]) are clearly visualized by reformatting of the 4D MUSIC data acquired in an 8-month-old 7-kg boy with complex congenital heart disease. The multiphase data have 0.9-mm isotropic resolution. Ao, aorta. From Han et al. [34], with permission from Wiley.

positive and negative predictive values, and accuracy of MRA were 82, 90, 88, 86, and 87% respectively. These studies indicate that whole-heart coronary MRA is useful in ruling out significant CAD in patients with suspected CAD. Kato et al. reported [39] their multicenter trial with a 3D, navigator-corrected SSFP whole-heart coronary MRA sequence at 1.5 T from seven centers in Japan. Of these multicenter coronary MRA studies, 92% were completed; the average imaging time was 9.5±3.5 min. The sensitivity was 88%, the specificity was 72%, and the positive and negative predictive values were 71 and 88% respectively.

Contrast-enhanced whole-heart coronary MRA at 3.0 T has emerged as a means of increasing the contrast-to-noise ratio compared with noncontrast 1.5-T whole-heart coronary MRA [6, 40, 41]. Contrast-enhanced whole-heart coronary MRA at 3.0 T now represents the current state-of-the-art technique. The diagnostic accuracy of 3.0-T contrast-enhanced whole-heart coronary MRA was evaluated in 69 patients with suspected CAD in our single-center trial [42]. Our study demonstrated that coronary MRA acquisition at 3.0 T was successful in 62 of 69 patients (90%), with the average acquisition duration being 9.0±1.9 min. Contrast-enhanced whole-heart coronary MRA at 3.0 T allows the ruling out of significant CAD with high sensitivity and moderate specificity. The sensitivity, specificity, and accuracy of whole-heart coronary MRA for detection of significant stenoses were 92% (87/95), 83% (570/686), and 84% (657/781) respectively, on a per-segment basis. Yang et al. also demonstrated a comparable diagnostic accuracy for the detection of CAD in 110 patients using similar imaging techniques with a 32-channel coil [43]. He et al. [44] reported in a preliminary study that the performance of a contrast-enhanced, self-navigated whole-heart coronary MRA technique has high sensitivity in detecting stenosis compared with our technique.

These results are also quite similar to the recent experience with 64-slice multidetector CT angiography in a multicenter study [39]. However, a meta-analysis suggests that coronary CT angiography has better sensitivity and specificity than coronary MRA and is therefore advantageous for detecting and ruling out clinically relevant coronary stenosis [45]. Despite its excellent diagnostic accuracy, coronary CT angiography has the disadvantages of requiring rapid injection of iodinated contrast medium and of exposing patients to ionizing radiation. In addition, blooming artifact from calcification leads to false positive diagnosis in many cases. MRA does not suffer from these artifacts caused by calcification, and coronary MRA can potentially depict the lumen of calcified coronary arteries.

Because of the use of contrast agent and the inversion recovery pulse, high-resolution 3D delayed enhancement MR images can be reconstructed from the 3-T contrast-enhanced coronary MRA images. This facilitates the 3D reformation in any slice orientation as well as precise quantification of the damaged tissue and the direct association of the infracted territory with the respective coronary artery lesion. The major advantage is that it allows fast and comprehensive assessment of both

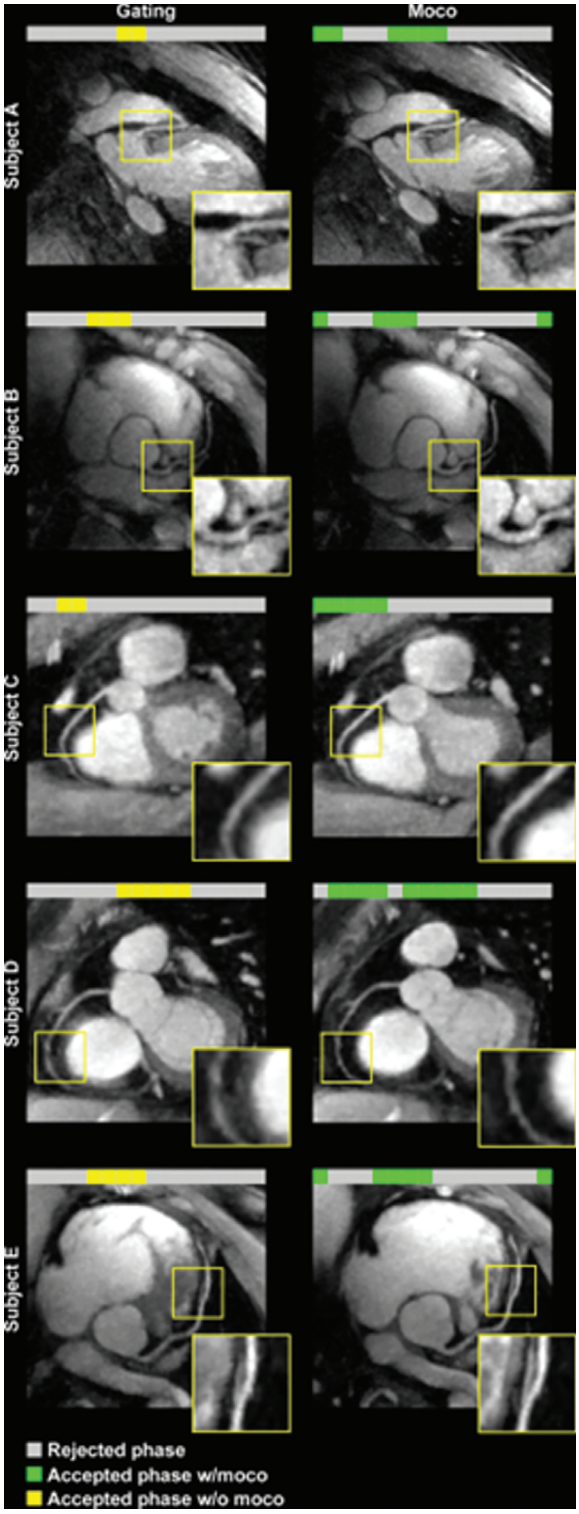

Figure 3 Example Images from Coronary Magnetic Resonance Angiography with Nonrigid Motion Correction. Five example subjects for comparison of conventional cardiac gating (*left*) with the proposed method (*right*). The proposed method with nonrigid motion correction significantly improved the quality of coronary visualization. moco, motion correction marked set by Yibin; w/moco, with motion correction; w/o moco, without motion correction marked set by Yibin. From Pang et al. [36], with permission from Wiley.

coronary artery stenosis and myocardial tissue damage in a single noninvasive and radiation-free test.

With recent technical advances, both multidetector CT and coronary MRA can provide lumenographic information about the coronary arteries to determine the presence and extent of CAD. Although spatial resolution needs to be further increased and the accuracy is not yet fully competitive with that of coronary CT angiography, coronary MRA has the potential to be a valuable adjunct in cases where coronary calcification precludes adequate evaluation or use of iodinated contrast agents is contraindicated. However, the functional implications of the lesion are more important. The combination of coronary MRA with tissue perfusion and viability provides a comprehensive assessment of the patient with known or suspected CAD without involving ionizing radiation. The use of blood-pool contrast agent might open the door to further increase the diagnostic accuracy of contrast enhanced coronary MRA at 3.0 T.

Coronary Vessel Wall and Plaque Imaging

Coronary vessel wall can be directly evaluated with MRI by elimination of the signal from luminal blood with use of various pulse sequence designs, known as dark-blood imaging. Through the use of different contrast mechanisms and various magnetization preparation methods, MRI has the capability of evaluating plaque size and characterizing plaque composition. Specific plaque features and activities that are related to its vulnerability, including fibrous cap integrity, lipid-rich/necrotic core, intraplaque hemorrhage, and inflammation, can be differentiated by various MRI methods [46]. However, most of the work in vessel wall MRI has been focused on the carotid artery, the aorta, and peripheral arteries. Coronary vessel wall MRI is still in the early stages of development because of motion, resolution, and scan time limitations.

Plaque Burden

Coronary plaque burden was demonstrated to be a stronger predictor of major adverse cardiovascular events compared with the severity of luminal stenosis. In a longitudinal study of 697 patients with acute

coronary syndromes, the cumulative rate of major adverse cardiovascular events was 20.4% after a median period of 3.4 years [47]. Multivariate analysis revealed that a baseline plaque burden (defined as plaque area divided by elastic membrane cross-sectional area) of 70% or greater was one of the independent predictors of subsequent major non-culprit lesion-related cardiovascular events. In a longitudinal study investigating the response to therapy in patients with acute coronary syndromes using cardiovascular MRI, 42 segments of coronary arteries from 22 patients were assessed at the baseline during the acute phase and 6 months after routine medical treatment with control of risk factors [48]. Coronary plaque burden was significantly reduced at 6 months after treatment compared with that at the baseline, and no significant changes were found in lumen area. A regression of vascular remodeling was also demonstrated because of the significant reduction in the wall-to-lumen ratio. Miao et al. [49] applied black-blood 2D coronary wall MRI in 179 patients in the Multi-Ethnic Study of Atherosclerosis and found coronary vessel wall positive remodeling in the asymptomatic subclinical atherosclerosis.

Technical development in MRI of plaque burden is focusing primarily on reducing the scan time, increasing the robustness to motion, extending the anatomical coverage with 3D acquisitions, and reducing the flow dependency. Ginami et al. [50] improved on conventional 2D double-inversion coronary wall MRI by incorporating golden angle acquisition, which allowed more flexible timing selection for optimal acquisition window. However, 2D acquisitions still suffer from user dependency in the placement of the imaging slice and poor resolution in the slice direction. Andia et al. [51] developed a 3D coronary wall imaging method based on subtraction of images with and without T2 preparation. The approach relies completely on the T2 relaxation differences between tissue types and therefore is flow independent. However, subtraction-based methods can be susceptible to motion sensitivity and incomplete fat suppression. Our group developed a method for 3D dark-blood vessel wall MRI using a local reinversion-based double-inversion scheme and interleaved gray blood images [52]. The additional gray blood contrast can potentially help identify superficial calcified nodules, although the scan time remains relatively long because of respiratory and cardiac gating. Cruz et al. [53] demonstrated the feasibility of nonrigid respiratory motion correction for speeding up the acquisition of 3D whole-heart vessel wall imaging.

Cardiovascular MRI has demonstrated its ability to visualize and quantify the increase or decrease in arterial vessel wall thickness and plaque burden and has been considered as a viable technology to assess therapeutic effects in clinical trials; however, only limited data are available on clinical application of cardiovascular MRI for the evaluation of coronary plaque burden. Further technical developments are needed to facilitate the clinical use and increase the robustness of this technique, and prospective studies in larger patient cohorts are still necessary to clarify the role of this noninvasive technique for the clinical diagnosis and assessment of CAD.

Intraplaque Hemorrhage and Thrombosis

Dark-blood T1-weighted MRI has been used to probe coronary intraplaque hemorrhage and thrombosis. Using a contrast mechanism similar to that used in the detection of carotid intraplaque hemorrhage [54], this technique is highly sensitive to target methemoglobin, a component of acute thrombus and hemorrhage that has a very short T1 relaxation time. Kawasaki et al. [55] first applied such a technique in patients with angina pectoris and at least 70% coronary stenosis on CT. They found that patients who demonstrated a significantly higher coronary plaque to myocardium signal intensity ratio (PMR) had a higher frequency of adverse plaque characteristics on CT, including higher positive remodeling and lower CT density. Oei et al. [56] examined CAD patients with this technique and also found that hyperintense plaques exhibited a significantly lower CT density. Jansen et al. [57] applied this technique in a small population with acute coronary syndrome and validated the MR findings by invasive angiography and thrombus histology. More recently, a prospective study with a much larger sample (568 patients with suspected or known CAD) led by Noguchi et al. [58] revealed that patients with hyperintensive plaque (PMR greater than 1.4) had a significantly higher likelihood (25.8%) of a subsequent coronary event compared with those with PMR between 1.0 and 1.4 (8.4%) and PMR less that 1.0 (1.1%). Multivariate regression analysis

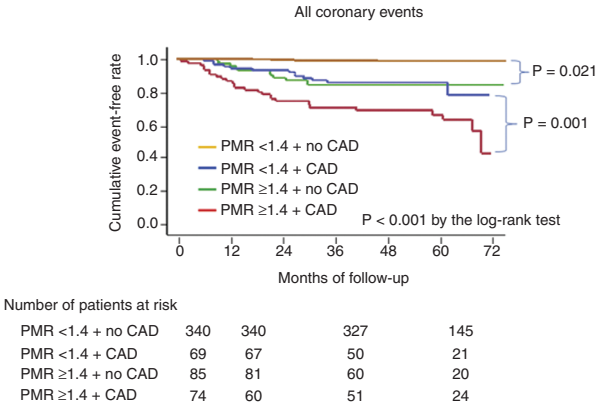

Figure 4 Kaplan-Meier Curves Comparing the Probability of All Coronary Events.
Coronary event-free survival was worst in the group with plaque-to-myocardium signal intensity ratios (PMRs) of 1.4 or greater and coronary artery disease (CAD) (*red line*) and best in the group with PMRs less than 1.4 but no CAD group (*orange line*). The rate in the group with PMRs of 1.4 or greater and no CAD (*green line*) was intermediate but comparable with that in the group with PMRs less than 1.4 and CAD (*blue line*). From Noguchi et al. [58], with permission from Elsevier.

also identified the elevation of PMR above 1.4 as the strongest independent predictor of major events during a 6-year follow-up (Figure 4). The same investigators also reported significant reduction in plaque hyperintensity in patients after 12 months of intensive statin therapy [59] (Figure 5). Our group found that hyperintensive plaques are associated with worse lipid profiles and high-risk plaque features observed by an invasive imaging technique [60] (Figure 6). It is important to note that hyperintensive plaques include not only intraplaque hemorrhage or thrombosis, but also many lipid-rich lesions as pointed out by Ehara et al. [61] in a study carefully comparing MRI with intracoronary optical coherence tomography. These findings form the basis for further larger-scale investigation into intervention trials and cost-effectiveness analysis to finally determine whether MR-depicted intraplaque hemorrhage and thrombosis may improve risk stratification and help identify patients who would more likely benefit from aggressive treatment.

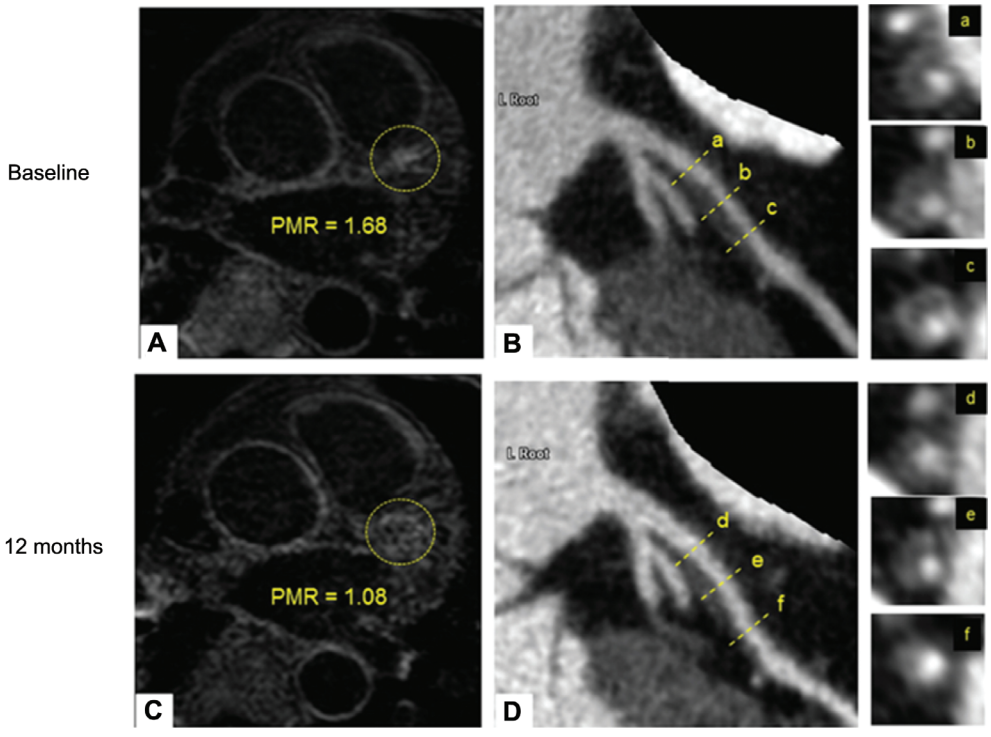

Figure 5 Plaque-to-Myocardium Signal Intensity Ratio (PMR) Regression with Statin Treatment.
A high-intensity plaque (HIP) with a PMR of 1.68 is observed in the proximal segment of the left anterior descending artery (LAD) at the baseline (*A*, *yellow dotted circle*). This HIP corresponds to the low-density coronary plaque with positive remodeling in the proximal portion of the LAD on computed tomography angiography (CTA; B). Cross-sectional CTA images of this HIP lesion show positive remodeling with low-attenuation plaque (LAP) (*a*, *b*, *c*). After 12 months of intensive statin treatment, PMR decreased to 1.08 (*C*, *yellow dotted circle*). CTA at follow-up shows a decrease in LAP volume (*D*, *d*, *e*, *f*). From Noguchi et al. [59], with permission from Elsevier.

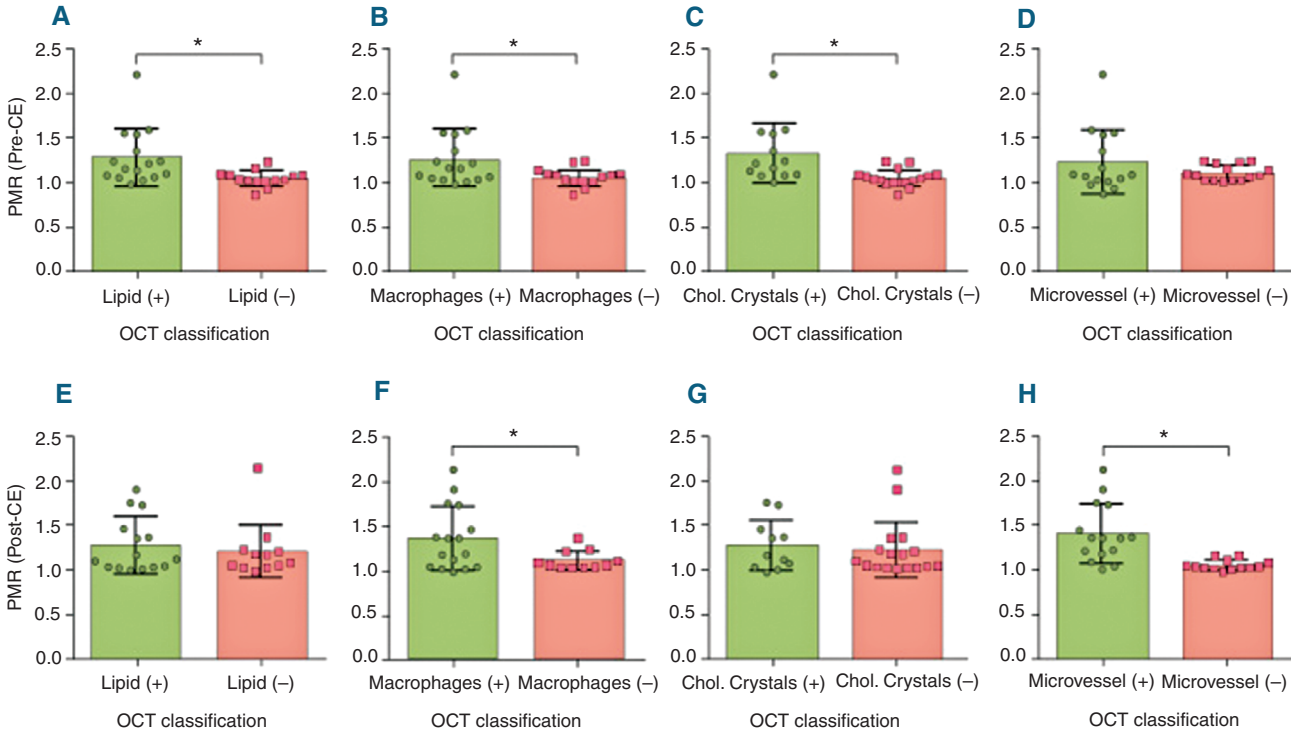

Figure 6 Relationship Between Plaque-to-Myocardium Signal Intensity Ratio (PMR) and Optical Coherence Tomography (OCT) Classifications.
Coronary plaques with high-risk features as classified by OCT tended to be hyperintensive on coronary atherosclerosis T1-weighted characterization with integrated anatomical reference images. (A–D) Precontrast PMR versus OCT classifications. (E–H) Postcontrast PMR versus OCT classifications. *Error bars* represent standard deviation. A *plus sign* and a *minus sign* denote lesion groups with corresponding OCT grading. *Asterisks* denote statistical significance ($P<0.05$). CE, contrast enhancement; Chol. cholesterol. From Xie et al. [60], with permission from Elsevier.

However, several technical limitations, including long scan time and low spatial resolution, restrict the clinical application of this imaging technique. Moreover, T1-weighted MRI heavily attenuates the signal from background tissue and requires co-registration with an additional coronary MRA to localize the hyperintensive plaque signal on the coronary vasculature. Further technical improvements are currently under development to address these limitations. For example, our group proposed a new MR technique with a motion-compensated interleaved acquisition scheme that provided both T1-weighted images and an integrated anatomical reference in a single scan [60] (Figure 7).

Vessel Wall Inflammation

Previous studies have revealed hyperenhancement within atherosclerotic plaques after the administration of gadolinium-based contrast materials by MRI [62–64]. Increased contrast enhancement is supposed to indicate the development of blood supply to the plaque (angiogenesis) as well as increased endothelial permeability. Thus contrast enhancement of plaque may act as a marker of plaque inflammation because the neovasculature growth into plaque and the increase of endothelial permeability, which promotes the transfer of the contrast material from the blood plasma to the plaque, strongly correlate with plaque inflammation [65]. Contrast enhancement patterns may also help differentiate different underlying pathological mechanisms. Varma et al. [66] studied the post-contrast images from CAD patients and patients with autoimmune inflammatory disease (systemic lupus erythematosus) and found that they had significantly greater total contrast-enhanced area than controls, with systemic lupus erythematosus patients showing a diffuse pattern and CAD patients showing patchy/regional contrast enhancement (Figure 8). In a different study with a comparable design, Schneeweis et al. [67] found

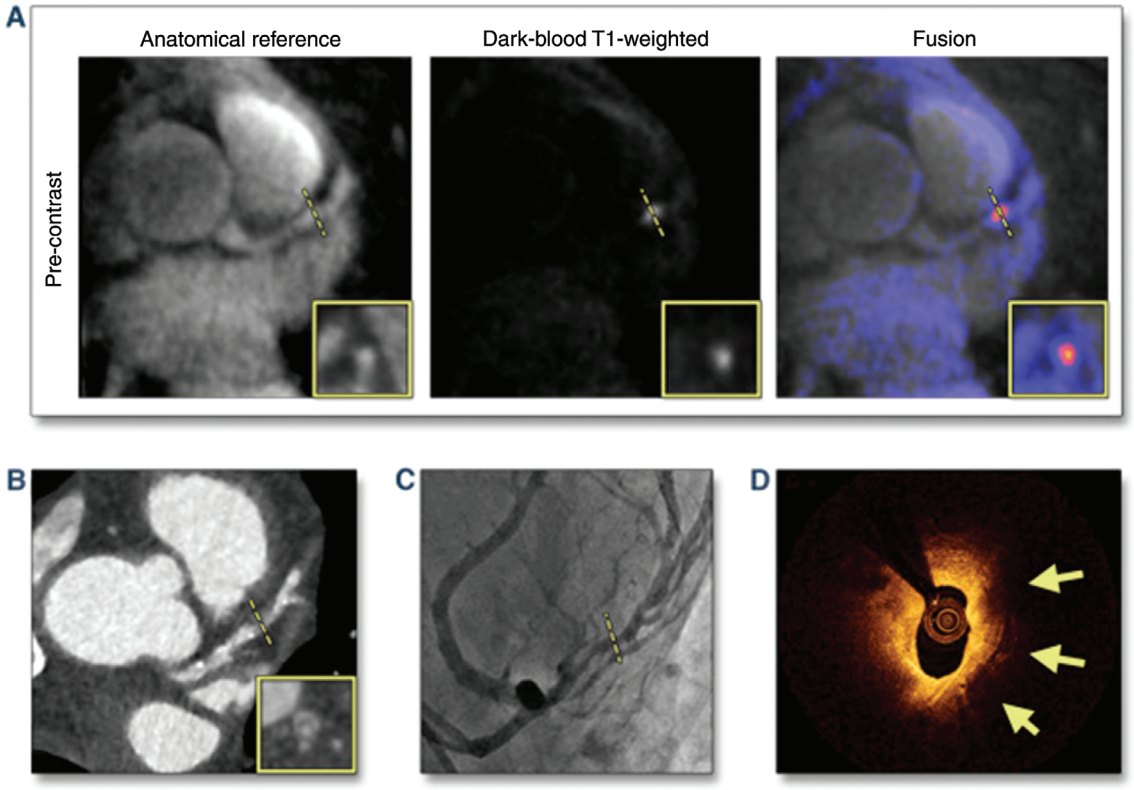

Figure 7 Representative Case of a Suspected Coronary Artery Disease Patient.
A coronary hyperintensive plaque (CHIP) was observed in the left anterior descending artery on coronary atherosclerosis T1-weighted characterization with integrated anatomical reference (CATCH). (A) Precontrast T1-weighted, anatomical reference, and fusion images. (B) Computed tomography angiography image. (C) X-ray angiography image. (D) Optical coherence tomography cross-sectional image at the corresponding location of the CHIP on CATCH. *Arrows* point to signal-poor regions, suggesting a large lipid pool. From Xie et al. [60], with permission from Elsevier.

common coronary enhancement in patients with Takayasu arteritis, similar to the pattern found in CAD patients. Lastly, it is important to note that the uptake of conventional gadolinium-based contrast agents is nonspecific and may represent chronic or acute inflammation as well as other related pathological conditions such as edema and fibrosis. The development of target-specific contrast agents is motivated to address this limitation [68, 69].

Vasomotor and Hemodynamic Functions

In addition to anatomical and pathological assessments, MRI provides the unique capability of measuring certain arterial physiological functions noninvasively, including vasomotor functions and reginal flow characteristics. Pepe et al. [70] reported their early experience of measuring the time course of endothelial-independent coronary vasodilation induced by nitroglycerin in healthy individuals using a 2D bright-blood technique with satisfactory reproducibility. Terashima et al. [71] demonstrated the clinical feasibility of a similar 2D MRA technique by applying it in a small patient population. An increase of 23% in the coronary cross-sectional area was observed as a response to induced vasodilation. The same group later reported a successful study in asymptomatic patients at high risk of CAD [72]. Patients with diabetes mellitus or end-stage renal disease showed impaired coronary vasodilation compared with age-matched controls. Using isometric handgrip exercise as an endothelial-dependent stressor, Hays et al. used an improved 3D MRA technique and successfully evaluated endothelial-dependent coronary vasoreactivity with amplified differences between healthy and diseased vessels in patients with CAD. Coronary vessel wall distensibility may also be evaluated by MRI, which is usually defined as the changes in lumen diameter or area during a cardiac cycle. Lin et al. [73] first

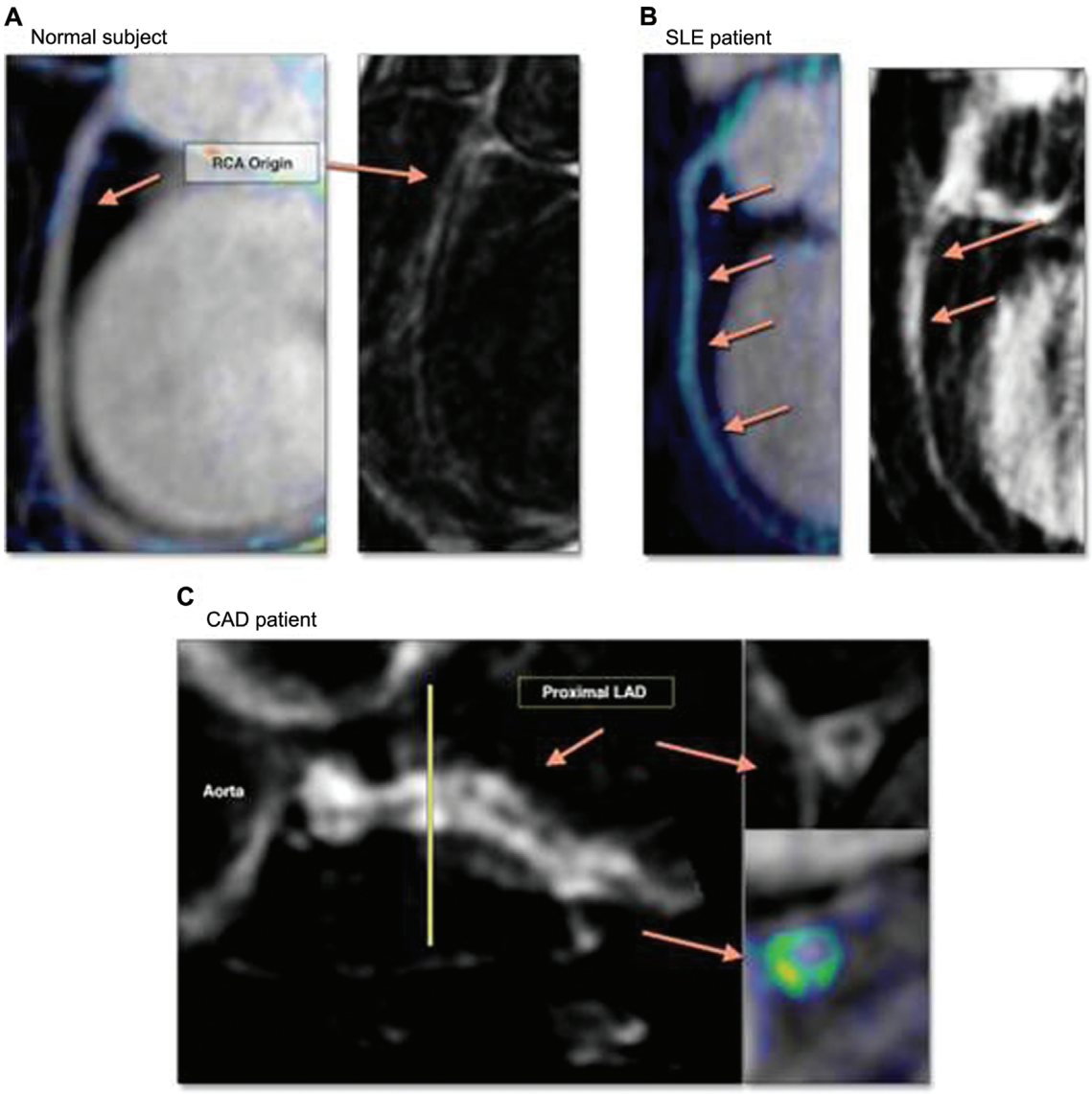

Figure 8 Representative Images of Clinical Findings with Contrast-Enhanced Magnetic Resonance Imaging. (A) Control subject (female, age 38 years) with mild right coronary artery (RCA) enhancement (*blue*). (B) A patient with systemic lupus erythematosus (SLE) (female, age 36 years), with generalized coronary enhancement over the projected long-axis view of the RCA. (C) A patient with coronary artery disease(CAD) (male, age 57 years), with patchy coronary enhancement within the area of soft plaque; short-axis view of the proximal part of the left coronary artery. LAD, left anterior descending artery. From Varma et al. [66], with permission from Elsevier.

studied the distensibility of coronary arteries using two 3D MRA images acquired in the middle of diastole and at the end of systole respectively. Coronary distensibility index was found to be significantly lower in patients with type 2 diabetes mellitus than that in control individuals.

The hemodynamics within the coronary circulation can be noninvasively quantified by phase-contrast MRI. Early pioneering studies by Hundley et al. [74] and Nagel et al. [75] demonstrated the feasibility of such a technique with intracoronary Doppler validation. The evaluation of coronary flow and coronary flow reserve has received renewed clinical interest thanks to the advent of fractional flow reserve (FFR) as the gold standard for determination of lesion-specific ischemia [76]. Our group has demonstrated the feasibility of measuring the pressure gradient across a coronary stenosis using 2D phase-contrast MRI. Patients with suspected CAD showed significant increase in the pressure difference compared with the controls. MRI-based FFR evaluation is in its infancy; technique

improvements and more rigorous clinical validation are required before it can be used to replace or supplement the invasive FFR methods.

The MR techniques used in the aforementioned studies are mostly based on conventional ECG-gated, respiratory navigator-gated or breath-hold acquisitions. Multiple 2D slices or 3D volumes with anisotropic voxel sizes are typically adopted to make the scan time short enough to be clinically feasible. These constraints undoubtedly limit the choice of the coronary segment that can be imaged and reduce the accuracy and reproducibility of the examinations. Nonetheless, MRI holds a unique advantage over other existing imaging methods for providing multifaceted functional information on the coronary pathophysiology. Importantly, MRI is well suited for serial measurements as it does not involve ionizing radiation or invasive procedures, making it ideal for evaluation of changes in coronary functions in response to therapeutic interventions. Since functional recoveries are likely to occur before morphological changes become detectable, the clinical impact of coronary MRI as a means for therapeutic monitoring is likely to surmount its existing technical shortcomings.

Conclusions

Coronary MRI is a noninvasive imaging modality that does not involve ionizing radiation. It uniquely possesses the versatility to provide multiparametric and potentially synergetic information on the disease status in the coronary arteries, such as luminal stenosis, plaque characteristics, endothelial functions, and flow. Rapid developments in coronary MRI techniques have resulted in significantly increased spatial resolution, image quality, reliability, and imaging speed, making MRI a more clinically feasible diagnostic tool for assisting in the management of CAD. More clinical evidence is emerging to demonstrate the added clinical value of coronary MRI.

Conflict of Interest

The authors declare no conflict of interest.

REFERENCES

1. Mendis S, Puska P, Norrving B. Global atlas on cardiovascular disease prevention and control. Geneva: World Health Organization in collaboration with the World Heart Federation and the World Stroke Organization, 2011.
2. Mozaffarian D, Benjamin EJ, Go AS, Arnett DK, Blaha MJ, Cushman M, et al. Heart disease and stroke statistics–2015 update: a report from the American Heart Association. Circulation 2015;131:e29–322.
3. Mendis S, Davis S, Norrving B. Organizational update: the world health organization global status report on noncommunicable diseases 2014; one more landmark step in the combat against stroke and vascular disease. Stroke 2015;46:e121–2.
4. Stehning C, Boernert P, Nehrke K. Advances in coronary MRA from vessel wall to whole heart imaging. Magn Reson Med Sci 2007;6:157–70.
5. Shea SM, Deshpande VS, Chung YC, Li D. Three-dimensional true-FISP imaging of the coronary arteries: improved contrast with T2-preparation. J Magn Reson Imaging 2002;15:597–602.
6. Bi X, Carr JC, Li D. Whole-heart coronary magnetic resonance angiography at 3 tesla in 5 minutes with slow infusion of Gd-BOPTA, a high-relaxivity clinical contrast agent. Magn Reson Med 2007;58:1–7.
7. Wang Y, Vidan E, Bergman GW. Cardiac motion of coronary arteries: variability in the rest period and implications for coronary MR angiography. Radiology 1999;213:751–8.
8. Wang Y, Watts R, Mitchell I, Nguyen TD, Bezanson JW, Bergman GW, et al. Coronary MR angiography: selection of acquisition window of minimal cardiac motion with electrocardiography-triggered navigator cardiac motion prescanning–initial results. Radiology 2001;218:580–5.
9. Danias PG, McConnell MV, Khasgiwala VC, Chuang ML, Edelman RR, Manning WJ. Prospective navigator correction of image position for coronary MR angiography. Radiology 1997;203:733–6.
10. Botnar RM, Stuber M, Kissinger KV, Manning WJ. Free-breathing 3D coronary MRA: the impact of "isotropic" image resolution. J Magn Reson Imaging 2000;11:389–93.
11. Bhat H, Ge L, Nielles-Vallespin S, Zuehlsdorff S, Li D. 3D radial sampling and 3D affine transform-based respiratory motion correction technique for free-breathing whole-heart coronary MRA with 100% imaging efficiency. Magn Reson Med 2011;65:1269–77.

12. Pang J, Bhat H, Sharif B, Fan Z, Thomson LE, LaBounty T, et al. Whole-heart coronary MRA with 100% respiratory gating efficiency: Self-navigated three-dimensional retrospective image-based motion correction (TRIM). Magn Reson Med 2014;71:67–74.
13. Stehning C, Börnert P, Nehrke K, Eggers H, Stuber M. Free-breathing whole-heart coronary MRA with 3D radial SSFP and self-navigated image reconstruction. Magn Reson Med 2005;54:476–80.
14. Piccini D, Littmann A, Nielles-Vallespin S, Zenge MO. Respiratory self-navigation for whole-heart bright-blood coronary MRI: methods for robust isolation and automatic segmentation of the blood pool. Magn Reson Med 2012;68:571–9.
15. Piccini D, Feng L, Bonanno G, Coppo S, Yerly J, Lim RP, et al. Four-dimensional respiratory motion-resolved whole heart coronary MR angiography. Magn Reson Med 2016. doi:10.1002/mrm.26221.
16. Ingle RR, Wu HH, Addy NO, Cheng JY, Yang PC, Hu BS, et al. Nonrigid autofocus motion correction for coronary MR angiography with a 3D cones trajectory. Magn Reson Med 2014;72:347–61.
17. Wu HH, Gurney PT, Hu BS, Nishimura DG, McConnell MV. Free-breathing multiphase whole-heart coronary MR angiography using image-based navigators and three-dimensional cones imaging. Magn Reson Med 2013;69:1083–93.
18. Luo J, Addy NO, Reeve Ingle R, Baron CA, Cheng JY, Hu BS, et al. Nonrigid motion correction with 3D image-based navigators for coronary MR angiography. Magn Reson Med 2016. doi:10.1002/mrm.26273.
19. Prieto C, Doneva M, Usman M, Henningsson M, Greil G, Schaeffter T, et al. Highly efficient respiratory motion compensated free-breathing coronary MRA using golden-step Cartesian acquisition. J Magn Reson Imaging 2015;41:738–46.
20. Moghari MH, Akçakaya M, O'Connor A, Basha TA, Casanova M, Stanton D, et al. Compressed-sensing motion compensation (CosMo): a joint prospective-retrospective respiratory navigator for coronary MRI. Magn Reson Med 2011;66:1674–81.
21. Akçakaya M, Basha TA, Chan RH, Manning WJ, Nezafat R. Accelerated isotropic sub-millimeter whole-heart coronary MRI: compressed sensing versus parallel imaging. Magn Reson Med 2014;71:815–22.
22. Forman C, Grimm R, Hutter JM, Maier A, Hornegger J, Zenge MO. Free-breathing whole-heart coronary MRA: motion compensation integrated into 3D cartesian compressed sensing reconstruction. Med Image Comput Comput Assist Interv 2013;16:575–82.
23. Nam S, Akçakaya M, Basha T, Stehning C, Manning WJ, Tarokh V, et al. Compressed sensing reconstruction for whole-heart imaging with 3D radial trajectories: a graphics processing unit implementation. Magn Reson Med 2013;69:91–102.
24. Pang J, Sharif B, Arsanjani R, Bi X, Fan Z, Yang Q, et al. Accelerated whole-heart coronary MRA using motion-corrected sensitivity encoding with three-dimensional projection reconstruction. Magn Reson Med 2015;73:284–91.
25. Luo J, Addy NO, Ingle RR, Hargreaves BA, Hu BS, Nishimura DG, et al. Combined outer volume suppression and T2 preparation sequence for coronary angiography. Magn Reson Med 2015;74:1632–9.
26. Henningsson M, Koken P, Stehning C, Razavi R, Prieto C, Botnar RM. Whole-heart coronary MR angiography with 2D self-navigated image reconstruction. Magn Reson Med 2012;67:437–45.
27. Bhat H, Ge L, Nielles-Vallespin S, Zuehlsdorff S, Li D. 3D radial sampling and 3D affine transform-based respiratory motion correction technique for free-breathing whole-heart coronary MRA with 100% imaging efficiency. Magn Reson Med 2011;65:1269–77.
28. Pang J, Bhat H, Sharif B, Fan Z, Thomson LE, LaBounty T, et al. Whole-heart coronary MRA with 100% respiratory gating efficiency: self-navigated three-dimensional retrospective image-based motion correction (TRIM). Magn Reson Med 2014;71:67–74.
29. Lai P, Bi X, Jerecic R, Li D. A respiratory self-gating technique with 3D-translation compensation for free-breathing whole-heart coronary MRA. Magn Reson Med 2009;62:731–8.
30. Aitken AP, Henningsson M, Botnar RM, Schaeffter T, Prieto C. 100% Efficient three-dimensional coronary MR angiography with two-dimensional beat-to-beat translational and bin-to-bin affine motion correction. Magn Reson Med 2015;74:756–64.
31. Schmidt JF, Buehrer M, Boesiger P, Kozerke S. Nonrigid retrospective respiratory motion correction in whole-heart coronary MRA, Magn Reson Med 2011;66:1541–9.
32. Ingle RR, Wu HH, Addy NO, Cheng JY, Yang PC, Hu BS, et al. Nonrigid autofocus motion correction for coronary MR angiography with a 3D cones trajectory. Magn Reson Med 2014;72:347–61.
33. Pang J, Sharif B, Fan Z, Bi X, Arsanjani R, Berman DS, et al. ECG and navigator-free four-dimensional whole-heart coronary MRA for simultaneous visualization of cardiac anatomy and function. Magn Reson Med 2014;72:1208–17.
34. Han F, Rapacchi S, Khan S, Ayad I, Salusky I, Gabriel S, et al. Four-dimensional, multiphase, steady-state imaging with contrast enhancement (MUSIC) in the heart: a feasibility study in children. Magn Reson Med 2015;74:1042–9.
35. Coppo S, Piccini D, Bonanno G, Chaptinel J, Vincenti G, Feliciano H, et al. Free-running 4D whole-heart self-navigated golden angle MRI: initial results. Magn Reson Med 2015;74:1306–16.
36. Pang J, Chen Y, Fan Z, Nguyen C, Yang Q, Xie Y, et al. High efficiency coronary MR angiography with

nonrigid cardiac motion correction. Magn Reson Med 2016;76:1345–53.
37. Sakuma H, Ichikawa Y, Suzawa N, Hirano T, Makino K, Koyama N, et al. Assessment of coronary arteries with total study time of less than 30 minutes by using whole-heart coronary MR angiography. Radiology 2005;237:316–21.
38. Sakuma H, Ichikawa Y, Chino S, Hirano T, Makino K, Takeda K. Detection of coronary artery stenosis with whole-heart coronary magnetic resonance angiography. J Am Coll Cardiol 2006;48:1946–50.
39. Kato S, Kitagawa K, Ishida N, Ishida M, Nagata M, Ichikawa Y, et al. Assessment of coronary artery disease using magnetic resonance coronary angiography: a national multicenter trial. J Am Coll Cardiol 2010;56:983–91.
40. Liu X, Bi X, Huang J, Jerecic R, Carr J, Li D. Contrast-enhanced whole-heart coronary magnetic resonance angiography at 3.0 T: comparison with steady-state free precession technique at 1.5 T. Invest Radiol 2008;43:663–8.
41. Prompona M, Cyran C, Nikolaou K, Bauner K, Reiser M, Huber A. Contrast-enhanced whole-heart MR coronary angiography at 3.0 T using the intravascular contrast agent gadofosveset, Invest Radiol 2009;44:369–74.
42. Yang Q, Li K, Liu X, Bi X, Liu Z, An J, et al. Contrast-enhanced whole-heart coronary magnetic resonance angiography at 3.0-T: a comparative study with X-ray angiography in a single center. J Am Coll Cardiol 2009;54:69–76.
43. Yang Q, Li K, Liu X, Du X, Bi X, Huang F, et al. 3.0T whole-heart coronary magnetic resonance angiography performed with 32-channel cardiac coils: a single-center experience. Circ Cardiovasc Imaging 2012;5:573–9.
44. He Y, Pang J, Dai Q, Fan Z, An J, Li D. Diagnostic performance of self-navigated whole-heart contrast-enhanced coronary 3T MR angiography. Radiology 2016;281:401–8.
45. Schuetz GM, Zacharopoulou NM, Schlattmann P, Dewey M. Meta-analysis: noninvasive coronary angiography using computed tomography versus magnetic resonance imaging. Ann Intern Med 2010;152:167–77.
46. Cai JM, Hatsukami TS, Ferguson MS, Small R, Polissar NL, Yuan C. Classification of human carotid atherosclerotic lesions with in vivo multicontrast magnetic resonance imaging. Circulation 2002;106:1368–73.
47. Stone GW, Maehara A, Lansky AJ, de Bruyne B, Cristea E, Mintz GS, et al. A prospective natural-history study of coronary atherosclerosis. N Engl J Med 2011;364:226–35.
48. Fernandes JL, Serrano CV Jr, Blotta MH, Coelho OR, Nicolau JC, Avila LF, et al. Regression of coronary artery outward remodeling in patients with non-ST-segment acute coronary syndromes: a longitudinal study using noninvasive magnetic resonance imaging. Am Heart J 2006;152:1123–32.
49. Miao C, Chen S, Macedo R, Lai S, Liu K, Li D, et al. Positive remodeling of the coronary arteries detected by magnetic resonance imaging in an asymptomatic population: MESA (Multi-Ethnic Study of Atherosclerosis). J Am Coll Cardiol 2009;53:1708–15.
50. Ginami G, Yerly J, Masci PG, Stuber M. Golden angle dual-inversion recovery acquisition coupled with a flexible time-resolved sparse reconstruction facilitates sequence timing in high-resolution coronary vessel wall MRI at 3 T. Magn Reson Med 2016. doi:10.1002/mrm.26171.
51. Andia ME, Henningsson M, Hussain T, Phinikaridou A, Protti A, Greil G, et al. Flow-independent 3D whole-heart vessel wall imaging using an interleaved T2-preparation acquisition. Magn Reson Med 2013;69:150–7.
52. Xie G, Bi X, Liu J, Yang Q, Natsuaki Y, Conte AH, et al. Three-dimensional coronary dark-blood interleaved with gray-blood (cDIG) magnetic resonance imaging at 3 tesla. Magn Reson Med 2016;75:997–1007.
53. Cruz G, Atkinson D, Henningsson M, Botnar RM, Prieto C. Highly efficient nonrigid motion-corrected 3D whole-heart coronary vessel wall imaging. Magn Reson Med 2016. doi:10.1002/mrm.26274.
54. Moody AR, Murphy RE, Morgan PS, Martel AL, Delay GS, Allder S, et al. Characterization of complicated carotid plaque with magnetic resonance direct thrombus imaging in patients with cerebral ischemia. Circulation 2003;107:3047–52.
55. Kawasaki T, Koga S, Koga N, Noguchi T, Tanaka H, Koga H, et al. Characterization of hyperintense plaque with noncontrast T1-weighted cardiac magnetic resonance coronary plaque imaging: comparison with multislice computed tomography and intravascular ultrasound. JACC Cardiovasc Imaging 2009;2:720–8.
56. Oei ML, Ozgun M, Seifarth H, Bunck A, Fischbach R, Orwat S, et al. T1-weighted MRI for the detection of coronary artery plaque haemorrhage. Eur Radiol 2010;20:2817–23.
57. Jansen CH, Perera D, Makowski MR, Wiethoff AJ, Phinikaridou A, Razavi RM, et al. Detection of intracoronary thrombus by magnetic resonance imaging in patients with acute myocardial infarction. Circulation 2011;124:416–24.
58. Noguchi T, Kawasaki T, Tanaka A, Yasuda S, Goto Y, Ishihara M, et al. High-intensity signals in coronary plaques on noncontrast T1-weighted magnetic resonance imaging as a novel determinant of coronary events. J Am Coll Cardiol 2014;63:989–99.
59. Noguchi T, Tanaka A, Kawasaki T, Goto Y, Morita Y, Asaumi Y, et al. Effect of intensive statin therapy on coronary high-intensity plaques detected by noncontrast T1-weighted imaging: the AQUAMARINE pilot study. J Am Coll Cardiol 2015;66:245–56.
60. Xie Y, Kim YJ, Pang J, Kim JS, Yang Q, Wei J, et al. Coronary atherosclerosis T1-weighed characterization with integrated anatomical reference: comparison with high-risk plaque features detected

by invasive coronary imaging. JACC Cardiovasc Imaging 2016. doi:10.1016/j.jcmg.2016.06.014.
61. Ehara S, Hasegawa T, Nakata S, Matsumoto K, Nishimura S, Iguchi T, et al. Hyperintense plaque identified by magnetic resonance imaging relates to intracoronary thrombus as detected by optical coherence tomography in patients with angina pectoris. Eur Heart J Cardiovasc Imaging 2012;13:394–9.
62. Weiss CR, Arai AE, Bui MN, Agyeman KO, Waclawiw MA, Balaban RS, et al. Arterial wall MRI characteristics are associated with elevated serum markers of inflammation in humans. J Magn Reson Imaging 2001;14:698–704.
63. Maintz D, Ozgun M, Hoffmeier A, Fischbach R, Kim WY, Stuber M, et al. Selective coronary artery plaque visualization and differentiation by contrast-enhanced inversion prepared MRI. Eur Heart J 2006;27:1732–6.
64. Yeon SB, Sabir A, Clouse M, Martinezclark PO, Peters DC, Hauser TH, et al. Delayed-enhancement cardiovascular magnetic resonance coronary artery wall imaging: comparison with multislice computed tomography and quantitative coronary angiography. J Am Coll Cardiol 2007;50:441–7.
65. Moulton KS, Vakili K, Zurakowski D, Soliman M, Butterfield C, Sylvin E, et al. Inhibition of plaque neovascularization reduces macrophage accumulation and progression of advanced atherosclerosis. Proc Natl Acad Sci U S A 2003;100:4736–41.
66. Varma N, Hinojar R, D'Cruz D, Arroyo Ucar E, Indermuehle A, Peel S, et al. Coronary vessel wall contrast enhancement imaging as a potential direct marker of coronary involvement: integration of findings from CAD and SLE patients. JACC Cardiovasc Imaging 2014;7:762–70.
67. Schneeweis C, Schnackenburg B, Stuber M, Berger A, Schneider U, Yu J, et al. Delayed contrast-enhanced MRI of the coronary artery wall in Takayasu arteritis. PLoS One 2012;7:e50655.
68. Phinikaridou A, Andia ME, Protti A, Indermuehle A, Shah A, Smith A, et al. Noninvasive magnetic resonance imaging evaluation of endothelial permeability in murine atherosclerosis using an albumin-binding contrast agent. Circulation 2012;126:707–19.
69. Botnar RM, Buecker A, Wiethoff AJ, Parsons EC Jr, Katoh M, Katsimaglis G, et al. In vivo magnetic resonance imaging of coronary thrombosis using a fibrin-binding molecular magnetic resonance contrast agent. Circulation 2004;110:1463–6.
70. Pepe A, Lombardi M, Takacs I, Positano V, Panzarella G, Picano E. Nitrate-induced coronary vasodilation by stress-magnetic resonance imaging: a novel noninvasive test of coronary vasomotion. J Magn Reson Imaging 2004;20:390–4.
71. Terashima M, Meyer CH, Keeffe BG, Putz EJ, de la Pena-Almaguer E, Yang PC, et al. Noninvasive assessment of coronary vasodilation using magnetic resonance angiography. J Am Coll Cardiol 2005;45:104–10.
72. Nguyen PK, Meyer C, Engvall J, Yang P, McConnell MV. Noninvasive assessment of coronary vasodilation using cardiovascular magnetic resonance in patients at high risk for coronary artery disease. J Cardiovasc Magn Reson 2008;10:28.
73. Lin K, Lloyd-Jones DM, Liu Y, Bi X, Li D, Carr JC. Noninvasive evaluation of coronary distensibility in older adults: a feasibility study with MR angiography. Radiology 2011;261:771–8.
74. Hundley WG, Lange RA, Clarke GD, Meshack BM, Payne J, Landau C, et al. Assessment of coronary arterial flow and flow reserve in humans with magnetic resonance imaging. Circulation 1996;93:1502–8.
75. Nagel E, Bornstedt A, Hug J, Schnackenburg B, Wellnhofer E, Fleck E. Noninvasive determination of coronary blood flow velocity with magnetic resonance imaging: comparison of breath-hold and navigator techniques with intravascular ultrasound. Magn Reson Med 1999;41:544–9.
76. Tonino PA, De Bruyne B, Pijls NH, Siebert U, Ikeno F, van't Veer M, et al. Fractional flow reserve versus angiography for guiding percutaneous coronary intervention. N Engl J Med 2009;360:213–24.